**Renu Ahlawat**[1]
**Vimal Chandra Srivastava**[1]
**Indra Deo Mall**[1]
**Shishir Sinha**[1]

[1]Department of Chemical Engineering,
Indian Institute of Technology Roorkee,
Uttarakhand, India.

Research Article

# Investigation of the Electrocoagulation Treatment of Cotton Blue Dye Solution using Aluminium Electrodes

This study was performed to investigate the variables that influence the removal efficiency of an acid dye, i.e., cotton blue (CB) (chemical name: aniline blue WS) dye, from aqueous solution by an electrocoagulation (EC) technique. Batch EC studies were performed using aluminum electrodes to evaluate the influences of various experimental parameters, i.e., initial pH ($pH_0$): 3–11, electrolysis time ($t$): 0–30 min, initial concentration ($C_0$): 100–1000 mg/L, electrode gap ($g$): 0.5–1.3 cm, number of electrodes ($N$): 4–10, and applied voltage ($V_{ap}$): 7–11 V, on the removal of CB dye. The optimum values of $pH_0$, $V_{ap}$ and $t$ for CB removal were found to be 6.0, 11 V and 15 min, respectively. The removal efficiency increased with decreasing values of $C_0$ and $g$. For a CB solution having $C_0$ = 100 mg/L, 97% removal efficiency was obtained at the optimized conditions. It was found that the EC sludge can be dried and thermally degraded. The bottom ash obtained after its combustion can be blended with cementitious mixtures. This approach for EC sludge disposal ensures energy recovery along with safe disposal of the EC sludge.

**Keywords:** Aniline blue WS; Decolorization; Electrocoagulation; Electrode gap; Sludge disposal; Textile dye

*Received:* January 26, 2008; *revised:* May 31, 2008; *accepted:* June 5, 2008

**DOI:** 10.1002/clen.200800019

## 1 Introduction

Textile industries generate considerable amounts of wastewater that contain strong colors, suspended organic and inorganic particles as well as having high pH and high chemical oxygen demand (COD). It is estimated that 1 to 15% of the dye is lost during dyeing and finishing processes due to the low dye fixation levels on the textile fibres [1, 2]. The disposal of colored wastewater is a cause of major environmental concern since colored effluent is undesirable not only from an aesthetic point of view, but it is also highly toxic. As a result, a significant amount of these dyes can exist in effluents from dyeing processes. Most synthetic dyes are toxic to human and aquatic life [3]. Adsorption, photo-degradation, biodegradation, membrane separation, chemical coagulation and electrocoagulation (EC) are the major techniques used for the removal of dyes from wastewater [4]. Adsorption with activated carbon is time-consuming and costly [5–7]. Photo-oxidation by ultraviolet (UV) rays in the presence of hydrogen peroxide ($H_2O_2$) or titanium dioxide ($TiO_2$) requires the use of additional chemicals. Although the biodegradation process is cheaper than other methods, it is less effective because of the inhibiting effect of toxic dyes on the bacterial development [8].

EC is an emerging water treatment technology that has been applied successfully to treat various wastewaters. It has been applied for treatment of potable water [9, 10], urban wastewater [11], heavy metal laden wastewater [12, 13], colored water [14], and pulp and paper mill wastewater [15, 16]. The advantages of EC over conventional technologies include high removal efficiency, compact treatment facility, and the possibility of complete automation. EC provides a simple, reliable and cost-effective method for the treatment of dye laden wastewater without the need for additional chemicals, and therefore, it avoids secondary pollution. The amount of sludge to be disposed in EC is lower compared to other dye removal processes [17].

The objective of the present study is to investigate the removal of cotton blue (CB) dye from aqueous solution via EC using aluminum as an electrode material. The effects of several parameters on the CB removal efficiency were investigated, i.e., initial pH ($pH_0$), inter-electrode distance ($g$), number of electrodes ($N$), applied voltage ($V_{ap}$), initial dye concentration ($C_0$), and electrolysis time ($t$).

## 2 Materials and Methods

### 2.1 Materials

Laboratory grade CB dye was obtained from Chemport India Private Limited. The characteristics of the dye are summarized in Tab. 1, and its molecular structure is shown in Fig. 1. Distilled water was used to prepare the desired concentration of CB solution. 1 g of dye was accurately weighed and was dissolved in 1 L distilled water to make a stock solution of 1 g/L. This stock solution was further

---

**Correspondence:** Prof. I. D. Mall, Department of Chemical Engineering, Indian Institute of Technology Roorkee, Roorkee, 247667, Uttarakhand, India.
**E-mail:** id_mall2000@yahoo.co.in

**Table 1.** Characteristics of cotton blue dye.

| Characteristics | Value |
|---|---|
| Chemical Name | Aniline Blue WS |
| Colour Index | 42755 |
| Chemical Formula | $C_{32}H_{25}N_3Na_2O_9S_3$ |
| Molecular Weight | 737.74 |
| Class | Triarylmethane |
| Solubility aqueous | Soluble |
| Hazardous Decomposition Products | Burning may produce carbon oxides (CO, $CO_2$), nitrogen oxides ($NO_x$), sulfur oxides. |
| pH (100 mg/L water) | 5.95 |
| $\lambda_{max}$ | 600 nm |

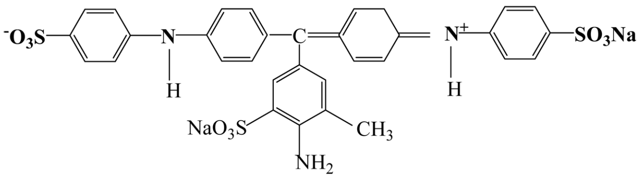

**Figure 1.** Molecular structure of cotton blue dye.

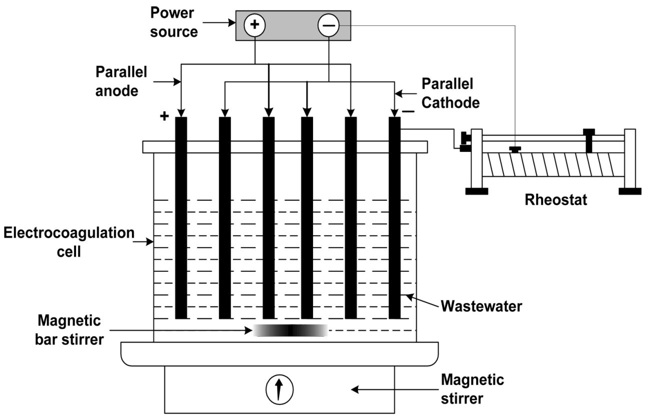

**Figure 2.** Schematic diagram of the experimental setup used for the electrocoagulation study.

diluted with distilled water to prepare dye solutions having concentrations in the range of 100 to 1000 mg/L.

## 2.2 Experimental Setup

The lab-scale batch experimental setup used for the EC studies is shown in Fig. 2. Experiments were carried out in a 1.5 L (10.8 cm × 10.8 cm × 13 cm) rectangular reactor made of perspex glass. Aluminum plates of 1 mm thickness were used as the electrodes. The electrode dimensions were 8 cm × 8 cm × 1 mm. The distance between two electrodes was varied in the range of 0.5 to 1.3 cm. The total effective surface area of each electrode was 64 $cm^2$, and a gap of 5 cm was maintained between the bottom of the electrodes and the bottom of the cell to facilitate easy stirring. Magnetic stirrers were used to agitate the solution. The electrodes were connected to a digital DC power supply (0–20 V, 0–5 A).

## 2.3 Experimental Procedure

The experiments were performed on dye solutions of known $C_0$ and $pH_0$. The pH the solutions was adjusted by adding 0.1 N sodium hydroxide (NaOH) or 0.1 N sulfuric acid ($H_2SO_4$) solutions. At the beginning of a run, 1.5 L of a solution of the desired concentration of the dye was fed into the reactor, and the power supply was switched on at $t = 0$. $V_{ap}$ was kept constant through the experiment. Samples were withdrawn at predetermined times (5–15 min), filtered and analyzed for the residual dye concentration.

A UV-VIS spectrophotometer (HACH, DR/5000) was employed to measure the CB dye concentration in the aqueous solution. A standard solution of the CB was scanned to determine the wavelength, $\lambda_{max}$, corresponding to maximum absorbance. The wavelength corresponding to maximum absorbance for CB was found to be 600 nm. The concentration of CB in the aqueous solution was estimated from the peak area of the absorption spectrum (300–900 nm) around $\lambda_{max}$, and by comparing the results to those of the known standard solutions. The percentage removal of CB was calculated using the following relationship, Eq. (1):

$$\text{Percentage removal } (\% R) = 100\,(C_0 - C_e)/C_0 \qquad (1)$$

where $C_0$ is the initial dye concentration (mg/L), and $C_e$ is the equilibrium dye concentration (mg/L).

## 2.4 Electrode and Sludge Analysis

Electrodes were removed from the EC reactor after a predetermined electrolysis time to determine the anode consumption. The aqueous solution was vigorously stirred, and the samples were analyzed for total aluminum using inductively coupled plasma mass spectrometry (ICP-MS, model ELAN-DRC-e). The forward power (radio frequency power) and extraction voltage (radio frequency voltage) of the ICP-MS were 1100 W and 200 V, respectively. The pressure of the argon gas used was 4 to 5 kg/$cm^2$ with a plasma gas flow rate of 15 L/min. The nebulizer gas flow and auxiliary gas flow rates were 0.93 and 1.2 L/min, respectively. The aluminum detection limit of ICP-MS was $5 \cdot 10^{-9}$ g/L (parts per trillion). The accuracy-reproducibility of the ICP-MS was 98 ± 1%.

Scanning electron micrograph (SEM) analysis of the aluminum electrodes was carried out before and after the EC treatment of CB solution using a LEO 435 VP scanning electron microscope. Thermogravimetric analysis (TGA) of the residues was carried out by using a Perkin Elemer (Pyris Diamond) thermogravimetric analyser. TGA scans were recorded from 25 to 1000°C using a scan rate of 10°C/min separately in both air and nitrogen atmospheres.

## 3 Results and Discussion

### 3.1 Effect of the Initial pH, ($pH_0$)

Various reactions take place in the EC reactor with aluminum as an electrode material. At the anode, metal ion generation takes place by the following reaction, Eq. (2):

$$Al\,(s) \rightarrow Al^{3+}(aq) + 3e^- \qquad (2)$$

In addition, oxygen evolution can compete with aluminum dissolution at the anode via the following reaction, see Eq. (3):

$$2H_2O\,(l) \rightarrow O_2\,(g) + 4H^+\,(aq) + 4e^- \qquad (3)$$

At the cathode, hydrogen evolution takes place via the reaction given in Eq. (4). It helps in the floatation of the flocculated particles out of the water.

$$3H_2O\,(l) + 3e^- \rightarrow 3/2H_2\,(g) + 3OH^-\,(aq) \qquad (4)$$

At high pH values, the $OH^-$ generated at the cathode during hydrogen evolution may attack the cathode by the following reaction, see Eq. (5) [18]

$$2\,Al + 6H_2O\,(l) + 2OH^- \rightarrow Al(OH)_4^- + 3H_2\,(g) \qquad (5)$$

$Al^{3+}$ and $OH^-$ ions generated via electrode reactions (2) and (4) react to form various monomeric species, e.g., $Al(OH)^{2+}$, $Al(OH)_2^+$, $Al_2(OH)_2^{4+}$ and $Al(OH)_4^-$, and polymeric species, e.g., $Al_6(OH)_{15}^{3+}$, $Al_7(OH)_{17}^{4+}$, $Al_8(OH)_{20}^{4+}$, $Al_{13}O_4(OH)_{24}^{7+}$, and $Al_{13}(OH)_{34}^{5+}$ [19]. The concentration of the hydrolyzed aluminum species depends on the aluminum concentration, and the solution pH. The speciation of $Al^{3+}$ ions in deionized water is presented in Fig. 3. The percentage of $Al^{3+}$ hydrolytic products was calculated from the following stability constants, see Eqs. (6–9) [20]:

$$Al^{3+} + H_2O \rightarrow Al\,(OH)^{2+} + H^+ \quad pK_1 = 4.95 \qquad (6)$$

$$Al\,(OH)^{2+} + H_2O \rightarrow Al(OH)_2^+ + H^+ \quad pK_2 = 5.6 \qquad (7)$$

$$Al(OH)_2^+ + H_2O \rightarrow Al(OH)_3 + H^+ \quad pK_3 = 6.7 \qquad (8)$$

$$Al(OH)_3 + H_2O \rightarrow Al(OH)_4^- + H^+ \quad pK_4 = 5.6 \qquad (9)$$

The hydrolysis constants for aluminum are 'squeezed' into an interval of less than 2 units. Therefore, apart from a narrow pH region of ca. 5–6, the dominant soluble species are $Al^{3+}$ and $Al(OH)_4^-$ at low and high pH values, respectively [21].

Canizares et al. [22, 23] carried out experiments to measure the chemical dissolution rate of aluminum electrodes at various pH. It was observed that the dissolution rate of aluminum was low at acidic pH followed by minima close to neutral pH. The dissolution rate was several orders of magnitude higher at alkaline pH ($pH > 11$) as compared to that at acidic or neutral pH. It was accompanied by formation of hydrogen bubbles from the sheet surface. This chemical dissolution of aluminum occurs via oxidation of the aluminum electrode with simultaneous reduction of water to form hydrogen. Chemical dissolution of the electrodes can be represented by following reaction, see Eq. (10) [18]:

$$2Al + 6H_2O\,(l) \rightarrow Al^{3+}(aq) + 3H_2\,(g) + 6OH^-\,(aq) \qquad (10)$$

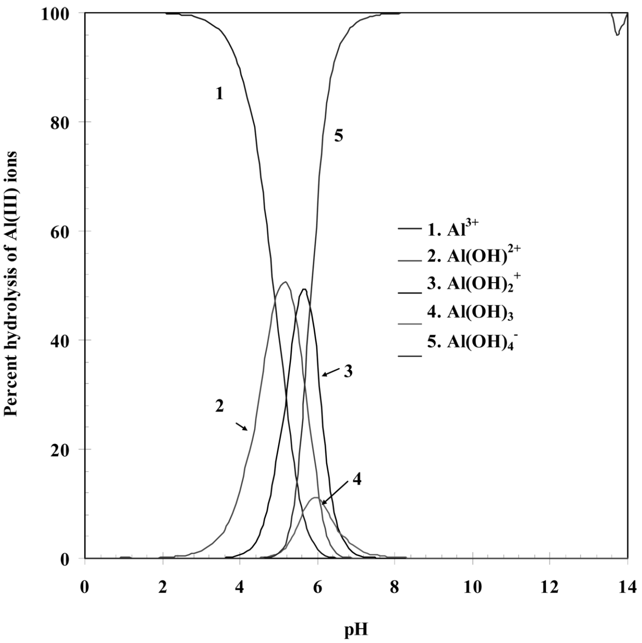

**Figure 3.** Speciation diagram of the $Al^{3+}$ ion.

There is a pH profile between the anode and the cathode in each electrochemical cell [22, 24]. On the anode, the water oxidation process, Eq. (3), generates a high concentration of protons, resulting in a lower pH, whereas, water reduction at the cathode, Eq. (4), results in the formation of hydroxyl ions and, hence, a higher pH. Therefore, the formation of coagulant on the surface of the cathode by chemical dissolution is of vital importance in EC reactors having aluminum electrodes. Hence, for aluminum-based EC reactors, super-faradic efficiencies are observed at $pH = 11.1$ [22].

In the present study, an attempt is made to investigate the influence of $pH_0$ on the EC process. The $pH_0$ value of the CB solution was varied in the range from 3.0 to 11.0. $pH_0 \geq 11$ was avoided since it was preferred to investigate the effect of $pH_0$ without super-faradic efficiencies. The original pH of the dye solution at $C_0 = 100$ mg/L in distilled water was 5.95. The results (figure not shown here) revealed that the removal at the original $pH_0$ was ca. 85.4%, and the CB removal efficiency was maximum and constant for $5.95 < pH_0 < 11.0$.

The pH was found to increase during the EC process, and stabilized at ca. 8.8 over the study range. This equilibrium pH represents a dynamic balance between the complex chemical reactions involving a $H^+$ or $OH^-$ donor and acceptor during EC. The outcome of the stable alkaline pH can be attributed to the cathodic water reduction, Eq. (4), being predominant over the anodic water oxidation, Eq. (3) and aluminium hydroxylation reactions, see Eqs. (6–9) [25].

For $pH_0 < 5.95$, the protons in the solution are reduced to $H_2$, and thus, the proportion of hydroxide ion produced is less. Consequently, there is a lower CB removal efficiency [26]. Precipitation and adsorption are the two major interaction mechanisms considered during the EC process. Each of the mechanisms is applicable at different pH ranges. At low pH values, metal species, e.g., $Al^{3+}$, generated at the anode bind to the anionic site of the dye molecules, thus neutralizing their charge and reducing their solubility. This process of removal is termed precipitation. The adsorption mechanism operates at higher pH ranges (pH > 6) and involves adsorption of organic substances on amorphous metal hydroxide precipitates [20, 27–29]. In the present case, for pH < 6, the primary mechanism is charge neutralization by monomeric cationic aluminum species, while for higher pH values, sweep coagulation with amorphous aluminum hydroxide explains the results [23].

## 3.2 Effect of Inter-Electrode Distance, (*g*)

Experiments were conducted by varying the value of the inter-electrode distance, *g*, and keeping all other parameters constant. It was found that when the value of *g* was increased from 0.5 to 1.3 cm, the CB removal efficiency decreased from 93.1 to 83.2%. For constant voltage supply, the electric current decreases with increasing values of *g*. This decreases the rate of release of $Al^{3+}$ ions leading to a lower interaction between dye molecules and the aluminum hydroxides produced during the EC, and thus, decreasing the CB removal efficiency at higher values of *g*.

## 3.3 Effect of Electrode Number, (*N*)

The CB removal efficiency was found to increase with an increasing values of the electrode number, *N*. As the value of *N* was increased from 4 to 10, the CB removal efficiency increased from 91.6 to 97.1%. Electrodes were in parallel connection, and therefore, higher values of *N* result in the formation of more EC cells within the reactor, leading to a higher release of $Al^{3+}$ ions, and hence, greater CB removal efficiency. In addition, the distribution of the coagulation agent density is more effective at higher values of *N*, and this increases the removal efficiency [30]. However, the efficiency increase slowed down at higher values of *N* due to lack of circulation of $Al^{3+}$ ions between the electrodes. For $N = 6$, the CB removal efficiency was found to be 95.8%.

## 3.4 Effect of Electrolysis Time, (*t*)

The dye removal efficiency depends directly on the concentration of ions produced by the electrodes, which in turn depends upon the electrolysis time, *t*. When the value of *t* increases, an increase occurs in the concentration of aluminum ions and their hydroxide flocs. Consequently, an increase in *t* increases the CB removal efficiency. An increase in *t* from 3 to 15 min was found to increase the removal efficiency from 69.5 to 97.1%. Further increases in *t* up to 30 min marginally increased the CB removal efficiency to 97.7%. It should be noted that the removal efficiency is also dependant on the concentration of the dye molecules requiring removal. For a solution having $C_0 = 100$ mg/L, the optimum value of *t* was found to be 15 min.

## 3.5 Effect of Applied Voltage, ($V_{ap}$)

The effect of applied voltage, $V_{ap}$, on the removal efficiency of the CB dye was also studied (figure not shown here). The maximum removal efficiency was 97% for a $V_{ap}$ value of 11 V for 15 min of treatment. The removal efficiency remained was almost constant for $V_{ap} > 11$ V. As the value of $V_{ap}$ increases, the efficiency of ion production on the anode also increases, and therefore, there is an increase in floc production in the solution, which results in an improvement in the CB removal efficiency.

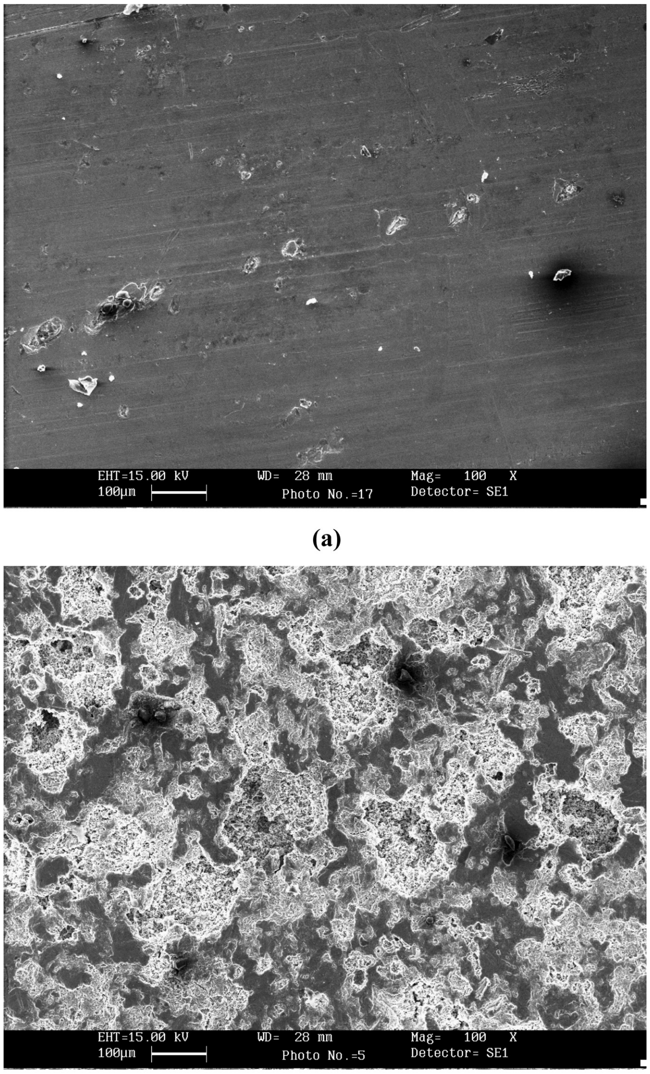

(a)

(b)

**Figure 4.** Scanning electron micrograph of aluminum electrode before and after electrocoagulation at 100x magnification. (a) Unused electrode, and (b) used electrode.

## 3.6 Effect of the Initial Dye Concentration, ($C_0$)

Experiments were conducted by varying the $C_0$ from 100 to 1000 mg/L in order to study the effect of $C_0$ on CB removal efficiency. Experiments performed at lower $C_0$ showed higher initial removal efficiency compared to the experiments with higher $C_0$. The CB removal efficiency decreased from 97% to 89% with an increase in concentration of the CB dye from 100 to 1000 mg/L. The effect of $C_0$ on the anode consumption was also studied. The anode consumption was found to increase from 0.092 to 0.144 g with an increase in $C_0$ from 100 to 1000 mg/L for 30 min of treatment. Thus, the anode consumption was not affected much by changes in $C_0$. Even when $C_0$ was increased 10-fold, the anode consumption only increased by one and half times the original value. Therefore, at higher $C_0$, the amount of hydroxide produced was not enough to remove all the dye molecules causing a decrease in the dye removal efficiency. In

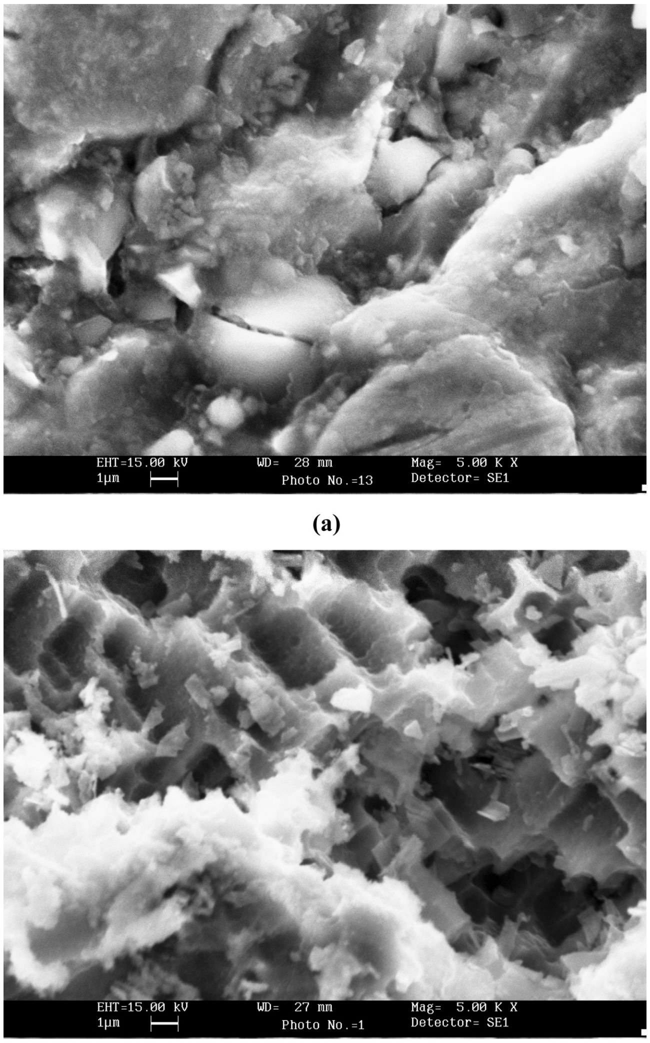

(a)

(b)

**Figure 5.** Scanning electron micrograph of aluminum electrode before and after electrocoagulation at 5000x magnification. (a) Unused electrode, and (b) used electrode.

addition, at higher $C_0$, $Al(OH)_3$ that forms near the surface, fouls the electrodes and intermediate products form in the solution, which block the electrode active sites. Both of these factors decrease the CB removal efficiency. With an increase in $C_0$, the resistance increases, and this leads to higher power consumption. It is quite clear that under the present experimental conditions, lower dye concentrations result in better dye removal efficiency [31].

## 3.7 SEM Analysis of the Electrodes

SEM images of aluminum electrodes, before and after, EC of CB dye solutions were obtained to compare the surface texture. Figure 4a) shows the original aluminum plate surface prior to its use in EC experiments. The surface of the electrode is uniform except for a few dents on the surface. Figure 4b) shows the SEM of the same electrode after several cycles of use in EC experiments. The electrode surface is now found to be rough, with a number of dents of ca. 10 to 100 μm in width and depth. These dents are formed around the nucleus of the active sites where the electrode dissolution results in the production of aluminum hydroxides. The formation of a large number of dents may be attributed to the anode material consumption at active sites due to the generation of oxygen at its surface. Figure 5 shows a magnified view of one such dent on the electrode surface, before and after, EC experiments. It can be seen that the dents in the electrode entrap degradation by-products such as micro-flocs and sludge particles. Thus, the active surface in the dent is blocked for further participation in the removal of dye [16].

## 3.8 Disposal and TGA Analysis of the Residues Collected Following the EC Experiments

The sludge generated during the EC process poses disposal and management problems. The recent environmental trends emphasize their utilization for some beneficial purpose and rendering them innocuous and benign to the environment. EC sludge can be dried and thermally degraded. The bottom ash obtained after its combustion can be blended with cementitious mixtures. Setting and leaching tests on the cementitious mixtures have shown that the bottom ash can be incorporated into the cementitious matrices to a great extent (75 wt% of total solid) without the risks of an unacceptable delay of cement setting and an excessive heavy metals leachability from the solidified products [32].

The principal experimental variables that affect the thermal degradation characteristics of solid residues in air and nitrogen flow are the pressure, the gas (purge gas) flow rate, the heating rate, the weight of sample and the sample size fraction. In the present study, the operating pressure was kept slightly positive, the purge gas (air or nitrogen) flow rate was maintained at 200 mL/min and the heating rate was maintained at 10°C/min.

The thermogravimetric analysis (TGA), differential thermal analysis (DTA) and differential thermal gravimetery (DTG) curves of the EC sludge in oxidizing and inert atmospheres at a heating rate of 10°C/min are shown in Figs. 6 and 7. The TGA traces for the residues in an oxidizing atmosphere, see Fig. 6, show the loss of moisture and the evolution of some light weight molecules including water (10% weight loss) from 25 to 100°C. Higher temperature drying (from 100–400°C) occurs due to loss of the surface bound water. The rate of weight loss was found to increase between ˜ 400 to ~570°C (~40% weight loss). This weight loss is generally associated with the evolution of $CO_2$ and CO. In the last temperature range between ~600–1000°C, residues oxidize and lose their weight gradually; and there is ~4% weight loss. The first derivative loss curve shows a strong exothermic peak centered between 400 to 600°C. This peak is due to the combustion of carbon species present in the sample. Thermal degradation characteristics in the flowing nitrogen atmosphere show moisture removal of ca. 10% up to 100°C followed by removal of light volatiles up to 1000°C. The residue left after heating in a nitrogen atmosphere up to 1000°C is ca. 48% of the original sample weight, and contains a greater proportion of fixed carbons along with a small amount of aluminum.

# 4 Conclusions

In the present study, electrocoagulation (EC) has been evaluated as a tool for cotton blue (CB) dye removal from aqueous solutions in a batch EC reactor with aluminum electrodes. The CB dye removal

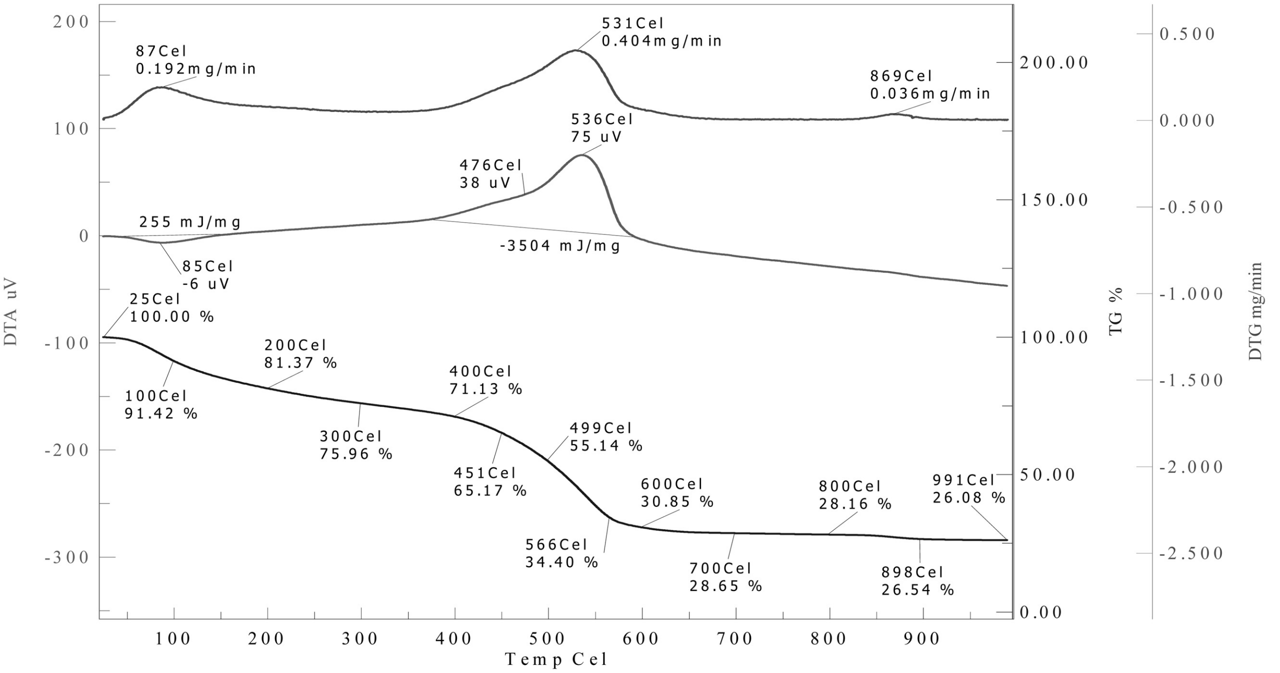

**Figure 6.** Thermal degradation analysis of EC sludge under flowing air.

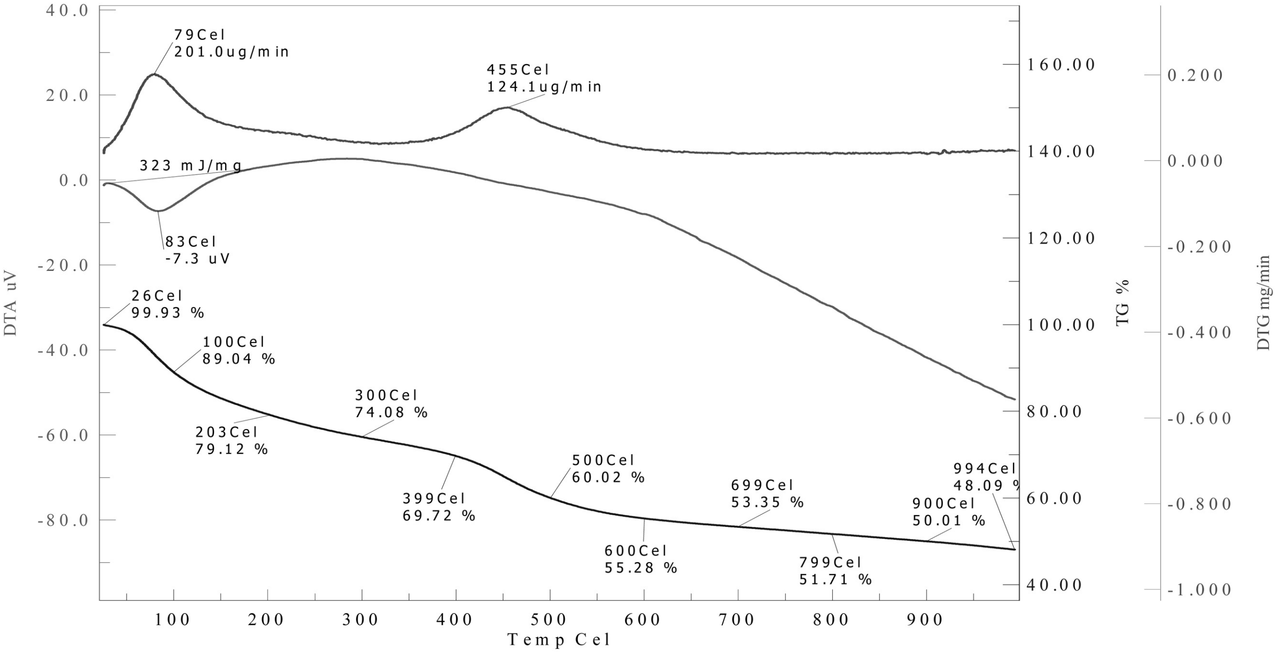

**Figure 7.** Thermal degradation analysis of EC sludge under flowing nitrogen.

was found to be affected by the initial pH ($pH_0$) of the solution, electrolysis time ($t$), initial concentration ($C_0$), inter-electrode distance ($g$), number of electrodes ($N$), and applied voltage ($V_{ap}$). The $pH_0$ was found to have a significant effect on removal efficiency and a maximum removal of 85.4% was observed at the optimum value of $pH_0 = 6$. For $pH_0 < 6$, the primary mechanism was charge neutralization by monomeric cationic aluminum species, while for higher values of $pH_0$, sweep coagulation with amorphous aluminum hydroxide explained the results. The CB removal efficiency increased with decreasing values of $g$, and with increasing values of $N$. The optimum values of $pH_0$, $t$, $g$, $N$, and $V_{ap}$ for CB removal were found to be 6.0, 15 min, 0.5 cm, 6, 11 V, and 15 min, respectively. For CB dye solution having an initial dye concentration of 100 mg/L, 97% dye removal was attained at the optimum conditions of treatment. It was also found in the present study that the EC sludge can be dried and thermally degraded. The bottom ash obtained after its combustion can be blended with cementitious mixtures. This approach for EC sludge disposal ensures energy recovery along with safe disposal of the EC sludge.

## Acknowledgement

The authors are grateful to the Ministry of Human Resources and Development, Government of India, for providing financial support to undertake this research work.

## References

[1] V. Mane, I. D. Mall, V. C. Srivastava, Kinetic and equilibrium isotherm studies for the adsorptive removal of brilliant green dye from aqueous solution by rise husk ash, *J. Environ. Manage.* **2007**, *84*, 390.

[2] V. Mane, I. D. Mall, V. C. Srivastava, Use of bagasse fly ash as an adsorbent for the removal of brilliant green dye from aqueous solution, *Dyes Pigm.* **2007**, *73*, 269.

[3] A. Alinsafi et al., Electrocoagulation of reactive textile dyes and textile wastewater, *Chem. Eng. Process.* **2005**, *44*, 461.

[4] T. Kim, P. Chulhwan, S. Eung-Bai, K. Sangyong, Decolorization of disperse and reactive dyes by continuous electrocoagulation process, *Desalination* **2002**, *150*, 165.

[5] I. D. Mall, V. C. Srivastava, N. K. Agarwal, I. M. Mishra, Adsorptive removal of malachite green dye from aqueous solution by bagasse fly ash and activated carbon- kinetic study and equilibrium isotherm analyses, *Colloids Surf., A* **2005**, *264*, 17.

[6] I. D. Mall, N. K. Agarwal, V. C. Srivastava, Adsorptive removal of Auramine-O: kinetic and equilibrium study, *J. Hazard. Mater.* **2007**, *143 (1–2)*, 386.

[7] I. D. Mall, V. C. Srivastava, G. V. A. Kumar, I. M. Mishra, Characterization and utilization of mesoporous fertilizer plant waste carbon for adsorptive removal of dyes from aqueous solution. *Colloids Surf., A* **2006**, *278 (1–3)*, 175.

[8] C. Allegre, P. Moulin, M. Maisseu, F. Charbit, Treatment and reuse of reactive dyeing effluents, *J. Membr. Sci.* **2006**, *269*, 15.

[9] E. A. Vik, D. A. Carlson, A. S. Eikum, E. T. Gjessing, Electrocoagulation of potable water. *Water Res.* **1984**, *18*, 1355.

[10] P. K. Holt, G. W. Barton, M. Wark, C. A. Mitchell, A quantitative comparison between chemical dosing and electrocoagulation, *Colloids Surf., A* **2002**, *211*, 233.

[11] M. T. Pouet, A. Grasmick, Urban wastewater treatment by electrocoagulation and flotation, *Water Sci. Technol.* **1995**, *31*, 275.

[12] D. Mills, A new process for electrocoagulation, *J. Am. Water Works Assoc.* **2000**, *92*, 35–43.

[13] K. Thella, B. Verma, V. C. Srivastava, K. K. Srivastava, Electrocoagulation study for the removal of arsenic and chromium from aqueous solution, *J. Environ. Sci. Health, Part A: Toxic/Hazard. Subst.* **2008**, *43 (5)*, 554.

[14] J. Q. Jiang et al., Laboratory study of electrocoagulation-flotation for water treatment, *Water Res.* **2002**, *36*, 4064.

[15] S. Mahesh, B. Prasad, I. D. Mall, I. M. Mishra, Electrochemical degradation of pulp and paper mill wastewater. Part 1. COD and color removal, *Ind. Eng. Chem. Res.* **2006**, *45*, 2830.

[16] S. Mahesh, B. Prasad, I. D. Mall, I. M. Mishra, Electrochemical degradation of pulp and paper mill wastewater. Part 2. Characterization and analysis of sludge, *Ind. Eng. Chem. Res.* **2006**, *45*, 5766.

[17] J. S. Do, M. L. Chen, Decolourization of dye-containing solutions by electrocoagulation, *J. Appl. Electrochem.* **1994**, *24*, 785.

[18] T. Picard, G. Cathalifaund-Feuillade, M. Mazet, C. Vandensteendam, Cathodic dissolution in the electrocoagulation process using aluminium electrodes, *J. Environ. Monit.* **2000**, *2*, 77.

[19] M. Bayramoglu, O. T. Can, M. Kobya, Decolorization of reactive dye solutions by electrocoagulation using aluminum electrodes, *Ind. Eng. Chem. Res.* **2003**, *42*, 3391.

[20] J. Duan, J. Gregory, Coagulation by hydrolyzing metal salts, *Adv. Colloid Interface Sci.* **2003**, *100*, 475.

[21] R. B. Martin, $Fe^{3+}$ and $Al^{3+}$ hydrolysis equilibria cooperativity in $Al^{3+}$ hydrolysis reactions, *J. Inorg. Biochem.* **1991**, *44*, 141.

[22] P. Canizares et al., Electrodissolution of aluminum electrodes in electrocoagulation processes. *Ind. Eng. Chem. Res.* **2005**, *44*, 4178.

[23] P. Canizares et al., Study of the electrocoagulation process using aluminum and iron electrodes, *Ind. Eng. Chem. Res.* **2007**, *46*, 6189.

[24] P. Canizares et al., Continuous electrocoagulation of synthetic colloid-polluted wastes, *Ind. Eng. Chem. Res.* **2005**, *44*, 8171.

[25] W. Den, C. Huang, H.-C. Ke, Mechanistic study on the continuous flow electrocoagulation of silica nanoparticles from polishing wastewater, *Ind. Eng. Chem. Res.* **2006**, *45*, 3644.

[26] N. Modirshahla, M. A. Behnajady, S. Kooshaiian, Investigation of the effect of different electrode connections on the removal efficiency of Tartrazine from aqueous solutions by electrocoagulation, *Dyes Pigm.* **2007**, *74 (2)*, 249.

[27] J. Gregory, J. Duan, Hydrolyzing metal salts as coagulants, *Pure Appl. Chem.* **2001**, *73*, 2017.

[28] A. Gurses, M. Yalcüin, C. Dogar, Electrocoagulation of some reactive dyes: a statistical investigation of some electrochemical variables. *Waste Manage.* **2002**, *22*, 491.

[29] O. T. Can, M. Bayramoglu, M. Kobya, Decolorization of reactive dye solutions by electrocoagulation using aluminum electrodes, *Ind. Eng. Chem. Res.* **2003**, *42*, 3391.

[30] N. Daneshvar, H. Ashassi-Sorkhabi, A. Tizpar, Decolorization of orange II by electrocoagulation method, *Sep. Purif. Technol.* **2003**, *31*, 153.

[31] M. Kobya, E. Demirbas, O. T. Can, M. Bayramoglu, Treatment of levafix orange textile dye solution by electrocoagulation, *J. Hazard. Mater.* **2006**, *B132*, 183.

[32] V. C. Srivastava, I. D. Mall, I. M. Mishra, Equilibrium modelling of single and binary adsorption of cadmium and nickel onto bagasse fly ash, *Chem. Eng. J.* **2006**, *117 (1)*, 79.